Addressing Two-Level Systems Variably Coupled to an Oscillating Field

Nir Navon,* Shlomi Kotler, Nitzan Akerman, Yinnon Glickman, Ido Almog, and Roee Ozeri

Department of Physics of Complex Systems, Weizmann Institute of Science, Rehovot 76100, Israel
(Received 27 October 2012; published 13 August 2013)

We propose a simple method to spectrally resolve an array of identical two-level systems coupled to an inhomogeneous oscillating field. The addressing protocol uses a dressing field with a spatially dependent coupling to the atoms. We validate this scheme experimentally by realizing single-spin addressing of a linear chain of trapped ions that are separated by $\sim 3~\mu$m, dressed by a laser field that is resonant with the micromotion sideband of a narrow optical transition.

Single-qubit addressing is a pristine form of quantum control, and is an increasingly important tool to probe and manipulate small-scale quantum registers. It is a necessary requirement for quantum computing schemes [1], while the use of single-spin imaging (and control) has recently allowed tremendous advances in the experimental study of quantum many-body systems [2]. One popular method relies on tightly focused fields, so as to have non-negligible coupling only to the target particle [3–5]. This scheme usually requires an optical transition, and application of an optical field on diffraction-limited length scales (or below [6]), which is very challenging due to stability reasons. Another general approach, inspired by magnetic resonance imaging, uses instead gradients of (electro)magnetic field. By lifting the energy degeneracy through a position-dependent Zeeman (or ac-Stark [7,8]) shift, single atoms can be addressed using the transition frequency that matches their location [9–14]. These schemes require either magnetic-field sensitive states or additional off-resonant levels to produce the ac-Stark shift. Yet another possibility arises if the addressing field can be engineered to have zero-coupling points, or commensurate values in the case of two particles, as proposed and demonstrated with micromotion addressing in ion traps [15,16].

In this Letter, we propose a general scheme for selectively addressing an array of two-level systems by using a spatially varying dressing field. The scheme has minimal requirements: it applies to perfect two-level systems (for which ac-Stark shift techniques are inefficient), and all frequencies necessary lie close to the transition frequency (contrary to **B**-field gradient methods, which use a dc component). In addition, the scheme is generic and works equally for optical, microwave, or radio frequency qubits, regardless of their magnetic-field sensitivity. Other systems could benefit from this scheme as various applications of dressed field control have been demonstrated for cold atomic gases [17], trapped ions [18], *NV* centers [19,20], or superconducting qubits [21]. We experimentally demonstrate this protocol using a linear array of trapped ions. The inhomogeneous dressing field was provided in our setup by the inhomogenous micromotion of ions in the

chain and a narrow linewidth laser that was tuned to the micromotion sideband of a narrow optical quadrupole transition.

We consider the Hamiltonian of the Rabi model, describing a noninteracting array of identical N two-level systems inhomogeneously coupled to an external oscillating field. The Hamiltonian for particle j reads

$$H_{\mathrm{lab}}^{(j)} = -\frac{\hbar\omega_0}{2}\sigma_z^{(j)} + \hbar\Omega_j\cos(\omega_L t)\sigma_y^{(j)}, \qquad (1)$$

where ω_L is the coupling field frequency, and $\sigma_i^{(j)}$ ($i = x$, y, z) is the i-Pauli matrix acting on particle j. Without loss of generality, the phase of the field is arbitrarily set to realize the σ_y coupling. Note that while the transition energy $\hbar\omega_0$ is assumed equal for all particles, the Rabi frequency associated with the coupling Ω_j is particle dependent. In the rotating-wave approximation (RWA), the Hamiltonian in the frame rotating at ω_L is

$$H_{\mathrm{dress}}^0 = \sum_j \frac{\hbar\Omega_j}{2}\sigma_y^{(j)} + \frac{\hbar\Delta}{2}\sigma_z^{(j)} = \sum_j E^{(j)}\sigma_{\phi_j}^{(j)}, \quad (2)$$

where the frequency detuning of the oscillating field to the atomic transition is $\Delta = \omega_0 - \omega_L$, $E^{(j)} = (\hbar/2) \times \sqrt{\Omega_j^2 + \Delta^2}$, and $\sigma_{\phi_j}^{(j)} = \sigma_y^{(j)}\cos\phi_j + \sigma_z^{(j)}\sin\phi_j$. The dressed states are the eigenstates of $\sigma_{\phi_j}^{(j)}$, with eigenenergies $\pm E^{(j)}$. It is thus possible to individually address particle j by inducing spin flips between the dressed states using a σ_x perturbation in the rotating frame, resonant with the dressed states transition energy. While for far off-resonant dressing fields ($\Delta \gg \Omega_j$) the energy difference between neighboring two-level systems drops as $\sim\Omega_i/\Delta$, optimal spectral distinguishability is obtained for $\Delta = 0$, i.e., for a resonant field with the transition. In that case, H_{dress}^0 is formally equivalent to the Hamiltonian of an array of spin-1/2 particles in a fictitious magnetic field pointing in the y direction and having a gradient along the axis of the ion crystal. In other words, the two-level systems are coupled to a spatially varying dressing field, and the
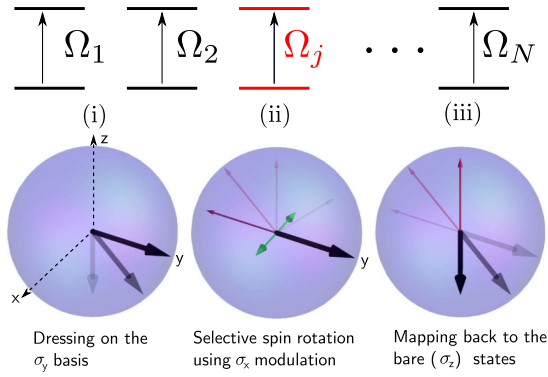
FIG. 1 (color online).   The system considered is an array of N identical noninteracting two-level systems, subjected to an external coupling field with a Rabi frequency Ω_j for particle j. The lower panel shows a sketch of the single-spin addressing protocol, involving three steps. (i) The bare eigenstates of all particles $\uparrow$ and $\downarrow$ at the Bloch sphere poles are mapped onto the dressed eigenstates in the sphere equatorial plane (shown by thick black arrows). (ii) A driving field (shown by the thin double green arrow) which is amplitude modulated at a frequency Ω_j rotates the spin of particle j (shown by the thin red arrow, and the red two-level system in the upper panel). (iii) The dressed states are mapped back on the bare basis at the sphere poles. All particles end up in state $\downarrow$, except particle j which is in $\uparrow$.

energies of the dressed states, which are the eigenstates of $\sigma_y^{(j)}$, are position dependent. Spectroscopic resolution can thus be mapped onto spatial resolution.

This analogy enables us to construct a simple protocol for individual spin rotations, as is illustrated in Fig. 1. (i) The bare spin eigenstates (σ_z basis) are mapped onto an eigenstate of the dressed spin (σ_y basis) $|\uparrow\rangle_d/|\downarrow\rangle_d$, and the strong resonant dressing field is turned on, locking the eigenstates in place by opening an energy gap between them. This energy gap is determined by the local coupling strength of each atom to the dressing field. (ii) A small σ_x perturbation is amplitude modulated (in the ω_0-rotating frame), with a modulation frequency δ, so that the Hamiltonian becomes $H_{\mathrm{dress}} = H_{\mathrm{dress}}^0 + \sum_{j=1}^N \hbar\lambda_j \cos(\delta t)\sigma_x^{(j)}$. This Hamiltonian is solved for each particle j by performing an additional change to a rotating frame, at an angular frequency Ω_j, assuming λ_j, $|\delta - \Omega_j| \ll \delta$, and neglecting the counterrotating terms in this frame of reference [22,23]. In that case, we readily find that the probability for spin j to be $|\uparrow\rangle_d$, while all the others are $|\downarrow\rangle_d$, is

$$P^{(j)}(t) = P_j(t)\prod_{l\neq j}[1 - P_l(t)], \qquad (3)$$

where $P_i(t) = [(\lambda_i/4\bar{\Omega}_i)^2\sin^2(\bar{\Omega}_i t/2)]$ is the Rabi precession, at a frequency $\bar{\Omega}_i = \sqrt{\Delta_i^2 + \lambda_i^2/4}$ and the detuning in the Ω_i-rotating frame is $\Delta_i = \Omega_i - \delta$. For all Ω_i's different from δ, the spins remain locked on the y axis while the spin of particle j is resonantly rotated around the x axis. (iii) The

dressed states are mapped back to the σ_z bare basis. Following this procedure, all particles remain in their initial state except for particle j, whose spin has been rotated.

We experimentally demonstrated the above individual spin-addressing scheme using a chain of atomic ions, held in a linear Paul trap, and typically separated by ~ 3 μm. The experimental setup is presented in detail elsewhere [24]. In short, we trapped and Doppler cooled one or more $^{88}\mathrm{Sr}^+$ ions in a linear Paul trap. We implemented a two-level system using the $5S_{1/2,+1/2}$ state, hereafter referred to as the bright state, due its photon statistics during state-selective fluorescence detection [25], and the long-lived $4D_{5/2,+3/2}$ state, hereafter called dark state. These two states are connected by an optical, electric-quadrupole, transition at 674 nm. This transition is driven using a narrow-linewidth diode laser stabilized to an external high-finesse cavity [25]. In an ideal linear Paul trap, the micromotion, due to the ac field modulated on the rf electrodes, vanishes along the symmetry axis of the trap. However, rather than a line of nulled rf amplitude as in the ideal case, the boundary conditions imposed by the trap end caps generate a linearly increasing rf amplitude around a null-amplitude point at the trap center [26]. The inhomogeneity of this excess micromotion along the chain is used as a spatially dependent coupling of the ions to the laser field. When operating the laser on the micromotion sideband of the quadrupole transition, located at a detuning of $\Omega_{\mathrm{rf}} = 21.75$ MHz from the carrier transition, the resulting Rabi frequency depends on the ion micromotion amplitude via $\Omega_j = \Omega_c J_1(\eta_j)$, where Ω_c is the carrier Rabi frequency, in the absence of modulation, J_1 is the first-order Bessel function of the first kind [27]. The parameter $\eta_j = \mathbf{k}\cdot\mathbf{x}_j$ is the micromotion Lamb-Dicke parameter of particle j along the laser wave vector $\mathbf{k}$, and $\mathbf{x}_j$ is its micromotion amplitude. For micromotion amplitudes small compared with the transition wavelength, $\eta_j \ll 1$, the local Rabi frequency can be approximated by $\Omega_j \approx \eta_j\Omega_c/2$. The micromotion amplitude of the ions in the chain can be controlled by applying a differential voltage to the trap end caps and displacing the ions along the trap axis, or by varying the rf voltage on the trap electrodes.

The values of the dressed state energies $\hbar\Omega_j$ for the different ions was first calibrated. The strength of the dressing field was measured through the frequency of the Rabi oscillations on the micromotion sideband for different end-cap voltages. For multispin systems, the population of ions in the dark state was estimated from photon detection histograms. Figure 2(a) shows the fraction of ions in the dark state versus the micromotion sideband pulse time, for a three-ion chain. The different Rabi frequencies involved can be conveniently extracted by Fourier analysis of the Rabi nutation curve, as shown in Fig. 2(b). Three frequencies, differing by roughly 5 kHz, are clearly observed. In Fig. 2(c), such spectra are shown as columns versus the global axial displacement of the chain.
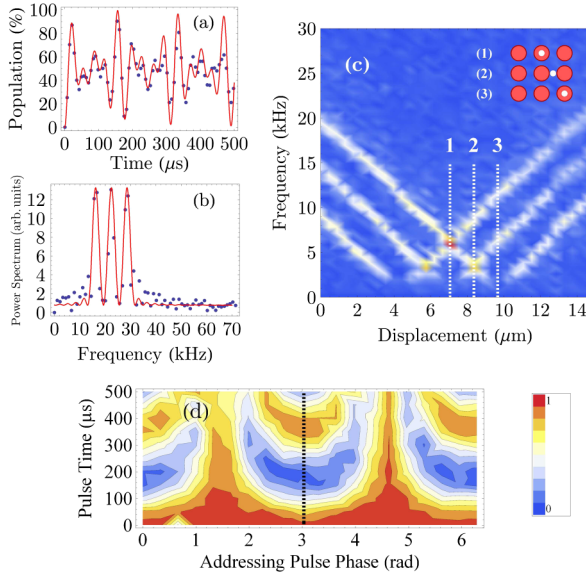
FIG. 2 (color online).   Calibration of the single-spin addressing protocol. Panels (a) and (b) show the time evolution and Fourier spectrum, respectively, of the fraction of dark ions in the three-ion chain driven on the micromotion sideband, for a given axial position of the chain. (c) Calibration of the dressed state energies by Fourier transform of the Rabi nutation curve on the micromotion sideband as a function of the axial displacement. The three particular points on the map (labeled 1–3) correspond to the rf null being, respectively, on the central ion, in between two rightmost ions, and on the rightmost ion, as shown in the schematic drawing on top of the map. The ions (rf null) are represented by red (white) disks. (d) 2D scan of the phase of the amplitude-modulated driving field (with respect to the dressing beam phase) and the pulse time for a single ion. A σ_x modulation is obtained for a phase $\phi \approx 3.03$ rad (vertical dashed black line).

As seen, the three frequencies shift linearly with the displacement. This linearity proves negligible effect of the spatial inhomogeneity of the laser beam profile on the dressed state energies on the length scales of Fig. 2. One frequency nulls every time one ion sits on the rf null [points labeled 1 and 3 in Fig. 2(c)].

In order to apply this scheme to a multispin system, one has to address simultaneously all spins for steps (i) and (iii). This can be solved in two different ways. (1) If micromotion is sufficiently weak so that the carrier Rabi frequency is almost constant throughout the chain, then one can apply a collective carrier $\pi/2$ pulse (along σ_x) to bring the spins to the equatorial plane, to match the dressed states. Here, the carrier and the micromotion sideband transitions, together with the rf signal for the trap electrodes, must all be phase locked. (2) The spins are set on the equatorial plane using rapid adiabatic passage (RAP) on the micromotion sideband interrupted on resonance. The RAP beam is kept on resonance, and thus automatically dresses the spins. In both schemes, following initialization, an amplitude-modulated-σ_x pulse rotates the spin of the particle of interest. After the single-spin rotation the

dressed states are mapped back to the bare states by reversing step (i). While we have successfully implemented both methods, we preferred the former, since RAP is several times slower than the carrier $\pi/2$ pulses.

The amplitude-modulated σ_x field was generated by adding a radio frequency, which was amplitude modulated at a frequency δ, to the laser acousto-optic modulator. This signal had the same carrier frequency and is phase shifted by $\pi/2$ from the dressing signal. Since the σ_y dressing and the σ_x driving field were provided by the same beam, $\lambda_i = \alpha \Omega_i$, and the Rabi frequency $\bar{\Omega}_i$ is proportional to Ω_i when the detuning Δ_i vanishes. The phase of the driving field was tuned in the following way. After the spins are dressed, the phase and time of the modulation are scanned, while the driving frequency δ is tuned to a single-spin resonance. The resulting spin-flip probability for a single ion is displayed in Fig. 2(d). The period of the pattern is π and we observed that at phases ϕ' and $\phi' + \pi$ (where $\phi' \approx 1.46$) the scan is independent of time, corresponding to a modulation collinear with the dressing field ($\phi = \pm y$). At phases $\phi' \pm \pi/2$ [vertical dashed line in Fig. 2(d)], we observe the highest contrast for the oscillations, corresponding to resonant σ_x rotations of the dressed state. Note that the sum of the σ_y dressing and the σ_x modulation could be equally well produced by direct frequency modulation of the σ_y beam.

We next scanned the frequency of the driving field 400 μs pulse. A typical spectrum, displayed in Fig. 3, exhibits three spectral features, corresponding to each ion addressed separately. The spectral splitting of the ions is given by the gradient of the coupling field, which in this case is proportional to the voltage applied on the rf electrodes. Using normal operation voltages, one easily reaches several kHz separation. This is an important figure of merit since small splittings require correspondingly longer pulses in order to frequency resolve the peaks. Comparing to the method of individual addressing using magnetic field gradients [10,11], the maximum splitting that we reached, of about 10 kHz, corresponds to a
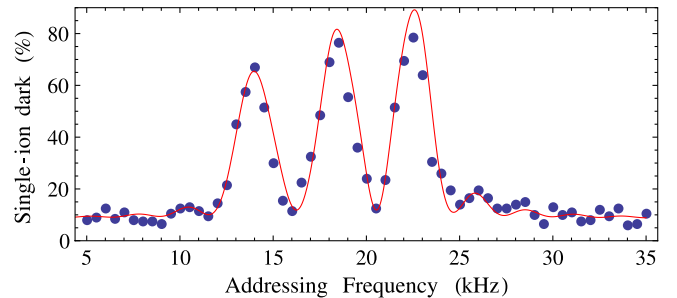

FIG. 3 (color online).   Spectrum of the single-addressing protocol for a three-ion chain taken after a pulse time of 400 μs, in a trap whose secular frequencies were $(\omega_x, \omega_y, \omega_z) = 2\pi \times (2.57, 2.45, 1.68)$ MHz. The rf frequency of the trap was 21.75 MHz.
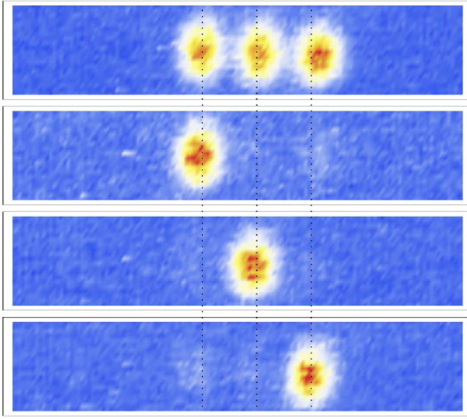
FIG. 4 (color online). Imaging the single-spin addressing pro-tocol on a three-ion chain. The inter-ion spacing is 3 μm. Each image below is an average of 50 pictures taken with an EMCCD camera, with an exposure time of 20 ms. In the upper image, all three ions are in the S state, and therefore fluoresce. In the lower images, a single ion remained in the S state while the other two were transferred to the D (dark) state. Because of the long exposure time required for the EMCCD imaging, there is a significant amount of error due to the finite lifetime of the dark state, in addition to the cross talk errors. For instance, on the second image, the error is, respectively, 7(4)% and 12(5)% for the central and rightmost ions, respectively.

magnetic field gradient of about 50 G/cm (assuming a magnetic field sensitivity of 2.8 MHz/G), which is similar to the one obtained in [11]. The Rabi frequency for each ion is easily deduced from a spectrum such as Fig. 3, taken with a different pulse time. For the 4 kHz splitting shown in Fig. 3, a π pulse of, respectively, 200, 280, and 560 μs leads to a spurious excitation of adjacent ions, which results from the overlap of their spectral response. The total cross talk error [28] is estimated from Eq. (3) to be, respectively, 1.6%, 1.1%, and 4.1% when addressing each ion respectively. The addressing fidelities of 90(2)%, 88(2)%, 85.6(2.5)% are consistent with an additional state preparation error per ion of 4%, due to the spin-lock efficiency limited at long holding times. This is also con-sistent with the fidelity reached in a two-ion chain, of 94(2)% (with π time of 180 μs). This limitation is not fundamental, and could be mitigated by increasing the power in the dressing field, or equivalently by increasing the rf voltage, both of which would increase the frequency gradient, and allow for shorter σ_x operations.

Finally, we verify the spatially selective nature of this protocol by taking images on an electron multiplying charge coupled device (EMCCD) camera. In the upper panel of Fig. 4, we show an image of a three-ion chain, where all the ions are in the bright state. We then selec-tively flip each ion spin using the above protocol, and average over 50 images. We indeed observe successful single-spin addressing. The faint "ghost" images of adja-cent ions are due to errors (see caption of Fig. 4).

In conclusion, we have presented a method to single-qubit address an array of two-level systems, using a dressing field and working exclusively with frequencies close to the two-level transition. As such, it could be adapted to various quantum systems. It is possible to extend the above protocol to prepare an arbitrary product state of single-qubit rotations. Indeed, while rotating spin j, particle i precesses at a constant frequency $\Omega_i - \delta$ around the y axis in the δ-rotating frame. In order to leave all particles ($\neq j$) state unchanged, one can apply a σ_x-spin echo when reaching half the pulse time of spin j. This would refocus all particles spin to their initial value while preparing particle j to its target state. With trapped ions, our protocol is well suited to address single ions in quantum registers using the typical intrinsic inhomogene-ity of micromotion in rf Paul traps and without any additional elements or any need for optical resolution. This technique could be useful with continuous density distributions as well, to select atoms with respect to their coupling to some external field. As an example, it could be used in atomic fountain clocks to select atoms accord-ing to their coupling to a microwave cavity, where the inhomogeneities arise from the microwave spatial mode, and would provide an additional knob to study collisional or cavity phase shifts.

Note added.—Recently, we became aware of a related work, realizing individual-ion addressing of a two-qubit chain using microwave field gradients on a microfabricated trap [29].

*Present address: Cavendish Laboratory, University of Cambridge, J. J. Thomson Avenue, Cambridge CB3 0HE, United Kingdom.
nn270@cam.ac.uk

[1] R. Blatt and C. Roos, Nat. Phys. **8,** 277 (2012).
[2] I. Bloch, J. Dalibard, and S. Nascimbene, Nat. Phys. **8,** 267 (2012).
[3] H. C. Nagerl, D. Leibfried, H. Rohde, G. Thalhammer, J. Eschner, F. Schmidt-Kaler, and R. Blatt, Phys. Rev. A **60,** 145 (1999).
[4] R. Dumke, M. Volk, T. Müther, F. B. J. Buchkremer, G. Birkl, and W. Ertmer, Phys. Rev. Lett. **89,** 097903 (2002).
[5] R. Scheunemann, F. S. Cataliotti, T. W. Hänsch, and M. Weitz, Phys. Rev. A **62,** 051801 (2000).
[6] C. Weitenberg, M. Endres, J. Sherson, M. Cheneau, P. Schauß, T. Fukuhara, I. Bloch, and S. Kuhr, Nature (London) **471,** 319 (2011).

[7] P. Staanum and M. Drewsen, Phys. Rev. A **66**, 040302 (2002).

[8] P. C. Haljan, P. J. Lee, K. A. Brickman, M. Acton, L. Deslauriers, and C. Monroe, Phys. Rev. A **72**, 062316 (2005).

[9] D. Schrader, I. Dotsenko, M. Khudaverdyan, Y. Miroshnychenko, A. Rauschenbeutel, and D. Meschede, Phys. Rev. Lett. **93**, 150501 (2004).

[10] S. Wang, J. Labaziewicz, Y. Ge, R. Shewmon, and I. Chuang, Appl. Phys. Lett. **94**, 094103 (2009).

[11] M. Johanning, A. Braun, N. Timoney, V. Elman, W. Neuhauser, and C. Wunderlich, Phys. Rev. Lett. **102**, 073004 (2009).

[12] A. Khromova, C. Piltz, B. Scharfenberger, T. F. Gloger, M. Johanning, A. F. Varon, and C. Wunderlich, Phys. Rev. Lett. **108**, 220502 (2012).

[13] N. Brahms, T. Purdy, D. Brooks, T. Botter, and D. Stamper-Kurn, Nat. Phys. **7**, 604 (2011).

[14] N. Lundblad, J. M. Obrecht, I. B. Spielman, and J. V. Porto, Nat. Phys. **5**, 575 (2009).

[15] Q. A. Turchette, C. S. Wood, B. E. King, C. J. Myatt, D. Leibfried, W. M. Itano, C. Monroe, and D. J. Wineland, Phys. Rev. Lett. **81**, 3631 (1998).

[16] D. Leibfried, Phys. Rev. A **60**, R3335 (1999).

[17] F. Gerbier, A. Widera, S. Folling, O. Mandel, and I. Bloch, Phys. Rev. A **73**, 041602 (2006).

[18] N. Timoney, I. Baumgart, M. Johanning, A. Varon, M. Plenio, A. Retzker, and C. Wunderlich, Nature (London) **476**, 185 (2011).

[19] C. Belthangady, N. Bar-Gill, L. M. Pham, K. Arai, D. Le Sage, P. Cappellaro, and R. L. Walsworth, Phys. Rev. Lett. **110**, 157601 (2013).

[20] J. M. Cai, B. Naydenov, R. Pfeiffer, L. P. McGuinness, K. D. Jahnke, F. Jelezko, M. B. Plenio, and A. Retzker, New J. Phys. **14**, 113023 (2012).

[21] C. M. Wilson, T. Duty, F. Persson, M. Sandberg, G. Johansson, and P. Delsing, Phys. Rev. Lett. **98**, 257003 (2007).

[22] B. Thimmel, P. Nalbach, and O. Terzidis, Eur. Phys. J. B **9**, 207 (1999).

[23] In the second RWA, all frequencies are of the same order of magnitude (in the kHz range), and one can thus expect some breakdown of the RWA.

[24] N. Akerman, Y. Glickman, S. Kotler, A. Keselman, and R. Ozeri, Appl. Phys. B **107**, 1167 (2012).

[25] A. Keselman, Y. Glickman, N. Akerman, S. Kotler, and R. Ozeri, New J. Phys. **13**, 073027 (2011).

[26] D. Berkeland, J. Miller, J. Bergquist, W. Itano, and D. Wineland, J. Appl. Phys. **83**, 5025 (1998).

[27] D. J. Wineland and W. M. Itano, Phys. Rev. A **20**, 1521 (1979).

[28] Starting with all particles in $|\downarrow\rangle_d$, the cross talk error when rotating the spin j to $|\uparrow\rangle_d$ is $1 - \max_t[P^{(j)}(t)]$. In other words, if any one particle state is incorrect, the result is an error regardless of whether or not the operation has been properly performed on the target qubit j.

[29] U. Warring, C. Ospelkaus, Y. Colombe, R. Jordens, D. Leibfried, and D. J. Wineland, Phys. Rev. Lett. **110**, 173002 (2013).